

Mixed-layer illite-vermiculite as a paleoclimatic indicator in the Pleistocene red soil sediments in Jiujiang, southern China



Ke Yin ^{a,*}, Hanlie Hong ^{a,b}, Gordon Jock Churchman ^c, Zhaojun Li ^d, Qian Fang ^a

^a Faculty of Earth Sciences, China University of Geosciences, Wuhan, Hubei 430074, China

^b Key Laboratory of Geobiology and Environmental Geology, the Ministry of Education, China University of Geosciences, Wuhan, Hubei 430074, China

^c School of Agriculture, Food and Wine, The University of Adelaide, 5005, Australia

^d Geosciences Department, University of Wisconsin – Parkside, Kenosha, WI 53141-2000, USA

ARTICLE INFO

Article history:

Received 28 January 2017

Received in revised form 26 June 2017

Accepted 30 June 2017

Available online 8 July 2017

Keywords:

Clay minerals

Pedogenesis

Mineralogy

Weathering

Climate

ABSTRACT

The mineralogy and chemical composition of the Jiujiang red soil sediments were investigated using X-ray diffraction (XRD), X-ray fluorescence (XRF), and inductively coupled plasma mass spectrometry (ICP-MS). Mixed-layer illite-vermiculite (I/V) was confirmed based on the conditions that a broad peak of 1.0 to 1.4 nm appeared in XRD after Mg-saturation, and its d-spacing did not change after glycol treatment, but collapsed to 1.0 nm after heating, owing to the loss of water and hydroxy-cations from its interlayer. The mixed-layer I/V contents fluctuate throughout the section but show a decreasing trend upwards, suggesting decreased weathering towards the surface of the section. The chemical index of alteration (CIA) values and Rb/Sr ratios also exhibit upward decreasing trends, jointly revealing the climate shift from warm/humid to cool/dry from the Middle to the Late Pleistocene. Although the general climate evolution can be evaluated by CIA values and Rb/Sr ratios, sub-climatic events within the Jiujiang red soil sediments cannot be identified. The $\text{SiO}_2/\text{Al}_2\text{O}_3$, $\text{Al}_2\text{O}_3/\text{Fe}_2\text{O}_3$, and $\text{SiO}_2/\text{Fe}_2\text{O}_3$ ratios clearly fluctuate along the section, especially within the net-like red soil sediments, but they do not reveal multiple climate cycles. This is because of an inhomogeneous distribution of SiO_2 , Al_2O_3 , and Fe_2O_3 in the white veins and the red matrix and also non-uniform sampling. The variation in the content of mixed-layer I/V show a strong positive correlation with changes in magnetic susceptibility of loess-paleosol sediments and in marine oxygen isotope ratios, revealing multiple sub-climate cycles on a global scale since the Middle Pleistocene. Therefore, the mixed-layer I/V contents not only reveal the whole climate trend documented in the red soil sediments since the Middle Pleistocene, but also disclose the sub-climate cycles related to the deposit-pedogenesis process.

© 2017 Elsevier B.V. All rights reserved.

1. Introduction

During deposition-pedogenesis processes, the pre-existing clay minerals in red soil sediments would transform to other clay types through a sequence of intermediate interstratified types with increasing degrees of weathering and changes in climatic conditions (Singer, 1980). Illite is usually considered as a little-altered detrital mineral derived from the existing bedrock or soil sediments (Millot, 1970; Weaver, 1989). However, the chemical leaching associated with weathering and climatic variations reduces the extent of alteration of illite (Bertsch and Thomas, 1985). Alteration of illite in soils has been most often reported to form vermiculite or hydroxyl-Al interlayered vermiculite (HIV), smectite, and kaolinite (Allen and Hajek, 1989; Bonifacio et al., 2009; Churchman, 1980; Churchman and Lowe, 2012; Ismail, 1970; Wilson, 2004; Yin et al., 2013). In sediments undergoing pedogenesis, mixed-

layer clays, such as mixed-layer illite-smectite (I/S), illite-vermiculite (I/V), illite-kaolinite (I/K) would form during the transformation of illite to smectite, vermiculite, and kaolinite, respectively (Bonifacio et al., 2009; Hong et al., 2014; Ren, 1988; Yin et al., 2013). I/V and I/S are metastable intermediate phases that would be more responsive to weathering and climate change than the end members V and S, as well as HIV, which is relatively insensitive because of interlayering with hydroxyl-Al species.

The well-known Quaternary loess-paleosol sequences over the loess plateau of northern China have been well studied and provide an unparalleled proxy record of Quaternary climatic changes (Chen et al., 1999; Kemp and Derbyshire, 1998; Kukla, 1987; Rutter et al., 1990). The red soil sediments widely distributed in the lower to middle reaches of the Yangtze River have similar grain-size distribution features to the loess deposits and are, therefore, believed to share a similar source provenance with the loess in the Chinese Loess Plateau (Hu et al., 2005; Li et al., 1997; Liu, 1985; Xiong et al., 2002; Yang et al., 1991). However, latest research on $^{143}\text{Nd}/^{144}\text{Nd}$ and $^{147}\text{Sm}/^{144}\text{Nd}$ ratios

* Corresponding author.

E-mail address: yinke1984@qq.com (K. Yin).

suggests that the red soil sediments from the Jiujiang section are derived from the drainage basins of the middle to lower Yangtze River (Hong et al., 2013a, 2013b). Subsequently, the fluvial sediments in southern China have experienced an intense chemical weathering under warm and humid tropical climate conditions. Like loess-paleosol sediments in the northern, the red soil sediments in southern China have also reflected the climatic and environmental changes occurring during their period of formation (Hu et al., 2005; Qiao et al., 2003; Yin and Guo, 2006; Zhao and Yang, 1995; Zhu et al., 2005). Previous studies of red soil sediments have focused on grain-size characteristics (Hu et al., 2005; Li et al., 1997), environmental magnetism (Hu et al., 2003; Zhao and Yang, 1995), and geochemical characteristics (Chen et al., 2008; Hong et al., 2009; Yang et al., 2004). Clay mineralogical investigations have also been undertaken on the Jiujiang and Xuancheng red soil sediments, and the changes in climatic conditions were revealed by variations in relative proportions of discrete clay minerals (Hong et al., 2009; Hong et al., 2013a, 2013b).

Mixed-layer I/V was found to be ubiquitous in all soil layers of the Jiujiang red soil sediments, with its contents fluctuating along the soil section. Red soil sediments in the Jiujiang section experienced syndepositional pedogenesis under humid tropical to subtropical conditions (Hu et al., 2010), and mixed-layer I/V formed from previous clay types during the syndepositional pedogenesis process (Hong et al., 2014). Thus, the pattern of mixed-layer I/V in the Jiujiang red soil sediments could provide a great opportunity to decipher paleoclimatic evolution during its formation. The presence of mixed-layer I/V from the upper Jiujiang section was confirmed by XRD analysis in previous investigations (Yin et al., 2013; Yin et al., 2014). Mixed-layer I/V was also detected in Xuancheng red soil sediments, and its genesis and paleoclimatic significance has been investigated (Hong et al., 2014). However, fewer studies have been conducted on the relationships between its variations and sub-climatic cycles during the Pleistocene. The sub-climatic cycles related to deposit-pedogenesis in the red soil sediments remain controversial, although some progresses on this problem have been made recently (Hu et al., 2003; Li et al., 1998; Yang et al., 1995).

The geochemistry reflects the climatic condition in the weathering process (Catt, 1991; Dal'Bó et al., 2010; Du et al., 2011; Kovács, 2007; Mahaney et al., 2014; Wilson, 1999). Hence, the geochemistry of paleosols is another powerful tool for interpreting pedogenical weathering processes and paleoclimatic conditions that are reflected in the soils. During weathering processes, mobile elements (e.g. K^+ , Ca^{2+} , and Na^+) are leached away more easily than the immobile elements (Al^{3+} and Ti^{4+}) (Nesbitt and Young, 1989). Thus, the relative variations of various elements can be used to assess the degree of chemical weathering and act as important indicators of the paleoclimatic evolution (Ji et al., 2004; Nesbitt et al., 1980; Nesbitt and Young, 1982; Qiao et al., 2011; Sheldon et al., 2002; Sheldon and Tabor, 2009). Elemental ratios such as SiO_2/Al_2O_3 , Al_2O_3/Fe_2O_3 , SiO_2/Fe_2O_3 , Rb/Sr , and the chemical index of alteration (CIA) can be used to evaluate the degree of chemical weathering in sediments with respect to their different mobilities during weathering (Chen et al., 1999; Hong et al., 2010; Nesbitt and Young, 1982).

Pleistocene sediments cover the middle to lower reaches of the Yangtze River in southern China. The Jiujiang red soil section is located in Jiujiang city, Jiangxi Province, in the zone of middle to lower reaches of the Yangtze River, southern China. Quaternary red soil sediments in Jiujiang were accretionary in nature and were subject to relatively intense syndepositional pedogenic alteration, reflecting the strengthening of both summer and winter monsoon circulations during their formation (Hong et al., 2013a, 2013b). Therefore, the investigation on the Jiujiang red soil sediments provides us a great opportunity to uncover the climatic evolution during the Quaternary. The goal of this study was to investigate the mineralogy of mixed-layer I/V and the chemical composition of the Pleistocene red soil sediments from the Jiujiang section using X-ray diffraction (XRD), X-ray fluorescence (XRF), and

inductively coupled plasma mass spectrometry (ICP-MS), with the aim of achieving an improved understanding of climatic evolution and multiple sub-climatic cycles in this region.

2. Materials and methods

2.1. Materials

The Jiujiang section ($29^{\circ}42'40.27''N$, $116^{\circ}00'13.7''E$) is one of the typical red soil sections in the middle to lower reaches of the Yangtze River (Fig. 1). The section is 14 m thick, and is lithologically divided into three units. The upper unit (0–3.2 m) is pale yellow to yellow-brown and contains minor amounts of Fe-Mn films and Mn nodules. The middle unit (3.2–6.2 m) is reddish to red-brown, containing sporadically pale yellow to grey spots and small short veins. The lower unit (6.2–14 m) is red-brown to dark-brown, characterized by well-developed white net-like veins that are more common and are relatively longer and wider than those in the middle unit. The middle and lower units have experienced much stronger weathering than the upper one (Hao et al., 2010).

The optical stimulated luminescence dating result of the sample at 0.8 m depth was $40.8 (\pm 4.9)$ ka, and the electron spin resonance dating results of samples at depths of 6.3, 8.1, 10.9, and 13.8 m were $393 (\pm 45)$, $452 (\pm 43)$, $592 (\pm 77)$, and $685 (\pm 65)$ ka, respectively. The oldest age of $685 (\pm 65)$ ka for the lowest red soil layer of the section indicates that the red soil formed after the mid-Pleistocene (Hong et al., 2013a, 2013b).

2.2. X-ray diffraction

The bulk sample was air-dried and then crushed manually to powder using an agate pestle and mortar. This powder sample was pretreated with 30% H_2O_2 overnight to remove organic materials. The clay mineral fraction ($<2 \mu m$) was obtained by sedimentation and centrifugation (Brown and Brindley, 1980). The clay mineral phase was determined by XRD analyses of the oriented air-dried, Mg-saturated, Mg-saturated and glycol solvated, and K-saturated samples. Mg-saturated and K-saturated samples were obtained by applying $MgCl_2$ and KCl solutions to air-dried mounts (Harris and White, 2008). Expansion properties of the sample were determined by Mg^{2+} saturation and glycol solvation (Velde and Meunier, 2008). The Mg-saturated and glycol-solvated sample was prepared by treating the Mg-saturated sample in a sealed container with ethylene glycol at $70^{\circ}C$ for 3 h (Hong et al., 2007). The air-dried K-saturated sample was analyzed at $25^{\circ}C$ and then heated successively to 110, 450, and $600^{\circ}C$ before analysis.

The XRD patterns of the clay samples were collected using a Panalytical X'Pert PRO DY2198 diffractometer at the Laboratory of Geological Process and Mineral Resources, China University of Geosciences (Wuhan). The instrument was operated at 40 kV and 40 mA with Ni-filtered $Cu K\alpha$ radiation. It was measured from 3° to $30^{\circ} 2\theta$ at a scan rate of $4^{\circ} 2\theta/min$ and a step size of $0.02^{\circ} 2\theta$. The abundances of clay minerals were estimated semi-quantitatively using the weight factor method (Olsen, 1998).

2.3. Major element analysis

All samples were first dried in an oven at $60^{\circ}C$ overnight and then ground to fine powder in an agate mortar. Prior to preparation of the fused pellets and measurement of loss-on-ignition (LOI), the samples were dried in an oven at $105^{\circ}C$ for 2 h. To measure LOI, 1 g of the dried sample was heated to $1000^{\circ}C$ for 1.5 h. The LOI value was calculated from the difference in weight between the sample heated to $1000^{\circ}C$ and to $105^{\circ}C$. For preparation of the fused pellets, 1 g of the dried sample powder was mixed with 5 g of dilithium tetraborate ($Li_2B_4O_7$). After homogenization, four drops of 1.5% LiBr were added into the sample. Pellets were pressed by a hydraulic press for 3 min at

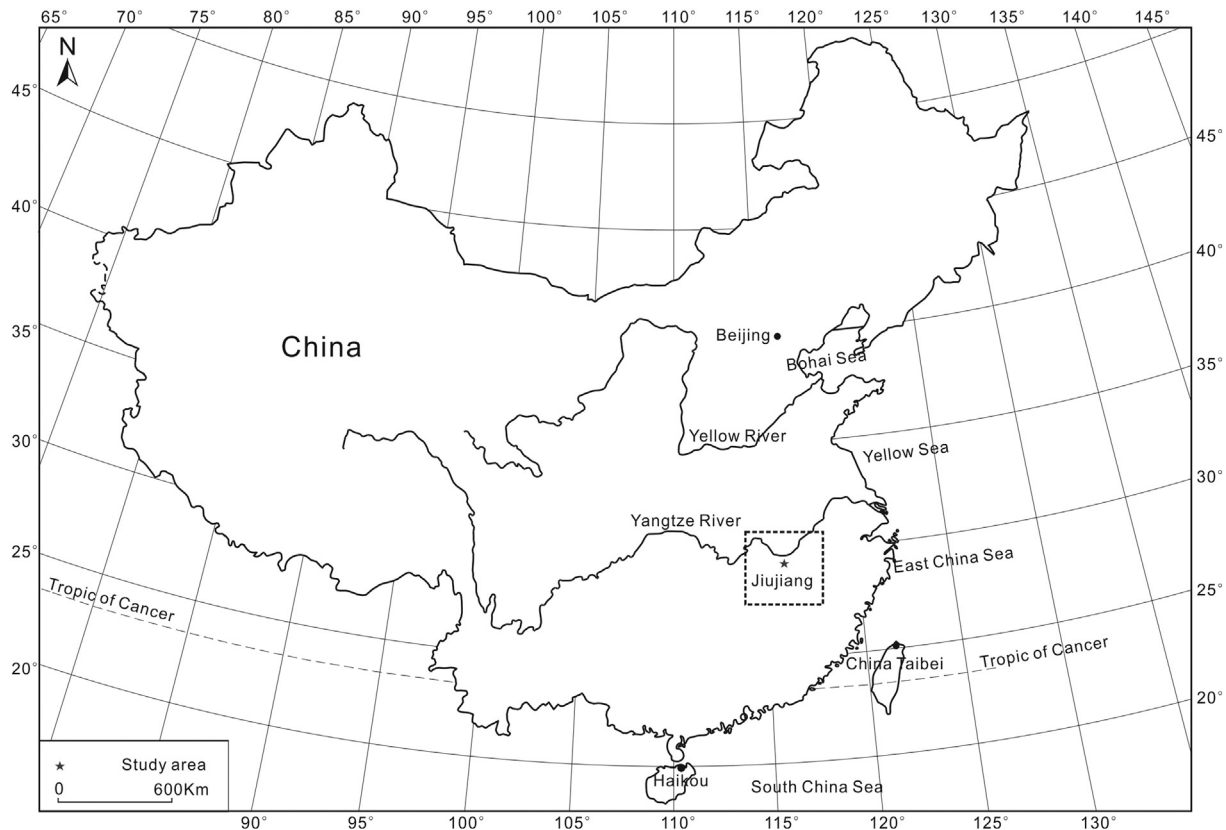


Fig. 1. A generalized map showing the location of the study area.

0.6 t/cm³ after 10 g of samples was mixed with 0.5 ml polyvinyl alcohol for 10 min. The fused pellets were then produced by Philips Perl' X3. Major element measurement was undertaken on an XRF-1800 SHIMADZU sequential X-ray fluorescence (XRF) spectrometer with a rhodium tube and a 2.5 kW generator at the State Key Laboratory of Biogeology and Environmental Geology of China University of Geosciences (Wuhan). The detection limit is ~0.01 wt% and analytical precision (relative standard deviation) is <1% for major elements except for H₂O.

In sediments forming soils, mobile elements would be lost and immobile elements would be enriched during weathering processes. The CIA index reflects the accumulation of the immobile element Al₂O₃ and the depletion of mobile elements CaO, K₂O, and Na₂O, and was used to characterize the degree of chemical weathering in the soil sediments (Nedachi et al., 2005; Nesbitt and Young, 1982). It is defined as the molar proportion ratio of Al₂O₃ to (Al₂O₃ + CaO* + Na₂O + K₂O), where CaO* is the amount of CaO in silicates, and provides a practical way to measure the chemical alteration of feldspars to clay minerals (Nesbitt and Young, 1982). Generally, SiO₂ is relatively more mobile than Al₂O₃ and Fe₂O₃ during the chemical weathering process (Chen et al., 1999), and SiO₂/Fe₂O₃, Al₂O₃/Fe₂O₃, and Al₂O₃/Fe₂O₃ ratios are also used to characterize the degree of weathering of a soil section (Hong et al., 2009).

2.4. Trace element analysis

Trace elements Rb and Sr were analyzed by ICP-MS (Agilent 7500a) at the State Key Laboratory of Geological Process and Mineral Resources of China University of Geosciences (Wuhan). The samples were digested in Teflon bombs with a mixture of HF + HNO₃ (Liu et al., 2008). The preparation procedure is briefly described as follows: ~50 mg sample powder was weighed into a Teflon bomb, moistened

with a few drops of ultra-pure water; 1.5 ml HNO₃ + 1.5 ml HF were added, the sealed bomb was heated to 190 °C in an oven for 48 h. The bomb was opened and the solution was allowed to evaporate to dryness at ~115 °C, followed by the addition of 1 ml HNO₃ and by evaporating again. The resultant salt was re-dissolved by adding ~3 ml of 30% HNO₃ and resealed and heated in the bomb at 190 °C for 12–24 h. The final solution was diluted to ~100 ml with a mixture of 2% HNO₃ for ICP-MS analysis.

Rb tends to be concentrated in K-feldspar, mica, and illitic minerals (Négrel, 2006), whereas Sr is preferentially hosted in Na- and Ca-rich minerals, such as carbonates, plagioclase, and amphibole (Chen et al., 1999). Carbonates as well as sodic and calcic aluminosilicates are more susceptible to weathering than K-containing minerals during pedogenesis, resulting in the depletion of Sr and the accumulation of Rb in paleosols (Chen et al., 1999). Therefore, the Rb/Sr ratio has been considered as a valid indicator for paleoclimatic changes during weathering and pedogenesis.

3. Results

3.1. X-ray diffraction

Illite, kaolinite, hydroxy-interlayered vermiculite (HIV), vermiculite, and minor mixed-layer I/V were identified in the previous investigations in the upper portion (Yin et al., 2013; Yin et al., 2014). A similar clay mineral assemblage was determined in the red soil sediments from the middle and lower portion (Fig. 2A–C). Mixed-layer I/V occurred universally along the Jiujiang section, with a vertical variation being found in the abundance of mixed-layer I/V (Fig. 3). Mixed-layer I/V was confirmed by the broad peaks ranging from 1.0 to 1.4 nm in Mg-saturated samples (Sawhney, 1989), with most diagnostic peaks occurring at ~1.20 nm. Glycol treatment does not alter the spacings, but

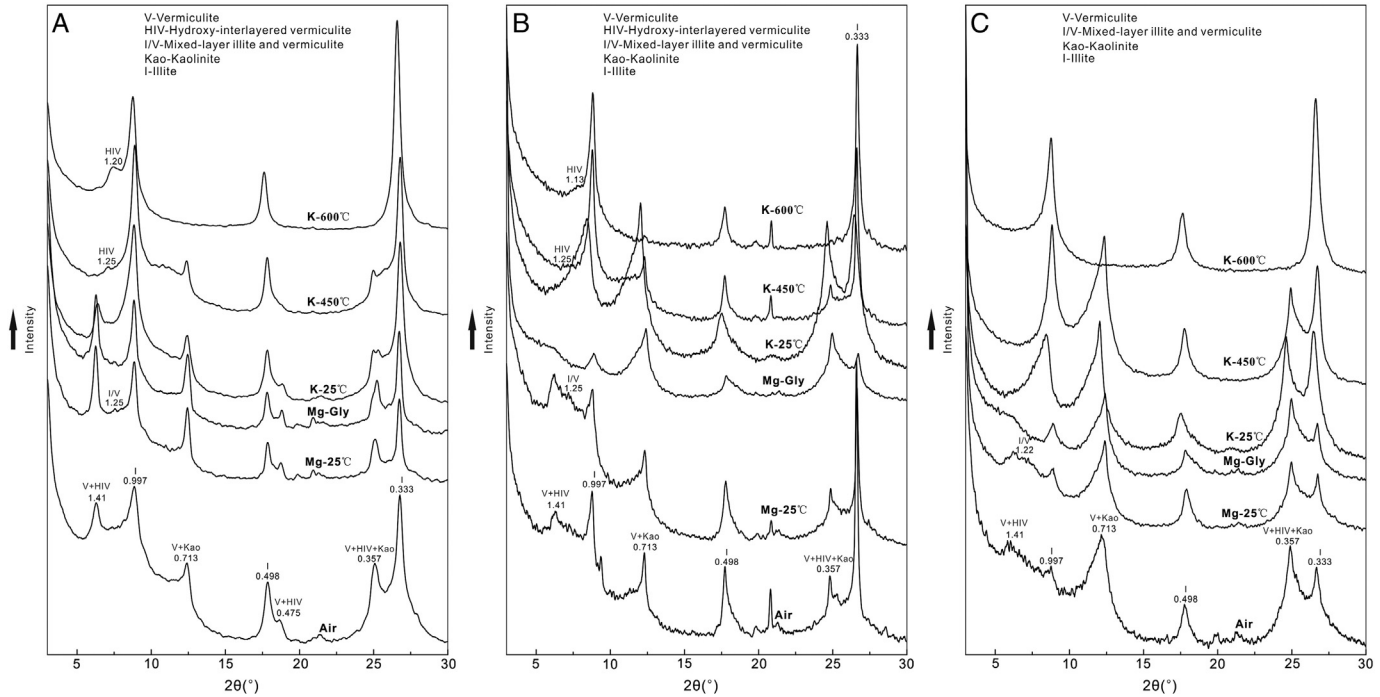


Fig. 2. The XRD patterns of representative samples showing the clay mineral composition (A, B, and C correspond to representative samples from the upper, the middle, and the lower portions of the Jiujiang red soil sediments, respectively). Air: Air-dried; Mg-25 °C: Mg-saturated at 25 °C; Mg-Gly: Mg-saturated and glycol solvation; K-450 °C: K-saturated and heated to 450 °C; K-600 °C: K-saturated and heated to 600 °C; V-vermiculite; HIV-hydroxy-interlayered vermiculite; I/V-mixed-layer illite and vermiculite; I-illite; Kao-kaolinite.

when the samples were K^+ saturated and heated to 110 °C, the layers of the vermiculite component collapsed to illite, resulting in a 1.0 nm peak and a series of higher orders. The peaks between 1.0 and 1.4 nm completely disappeared and the intensity of the 1.41-nm peak decreased significantly with increasing temperature. These phenomena are quite consistent with the behavior of mixed-layer I/V reported previously (Fagel et al., 1996; Lin et al., 2002). HIV was characterized by progressive but incomplete collapse of the (001) reflection after progressive thermal treatments and is prevalent in the upper portion of Jiujiang red soil sediments (Yin et al., 2013). Its abundance obviously decreases in the middle portion compared to the upper sediments (Fig. 2B), whereas, HIV is absent in the lower sediments (Fig. 2C). The obvious variations in HIV abundance might indicate different pedogenic conditions of the three soil units. Vermiculite was revealed by its non-expansion after Mg^{2+} saturation and glycol solvation and contraction in the K-saturated and air-dried state (Meunier, 2007; Velde and Meunier, 2008). The XRD patterns of Mg-saturated clay at 25 °C indicated that illite (1.0 nm and 0.333 nm peaks) and kaolinite (0.72 nm and 0.357 nm peaks) were present in the sediments (Fig. 2A–C).

3.2. Major element analysis

Changes in major chemical compositions of SiO_2 , Al_2O_3 , Fe_2O_3 , K_2O , TiO_2 , Na_2O , CaO , MgO , SiO_2/Al_2O_3 , Al_2O_3/Fe_2O_3 , SiO_2/Fe_2O_3 , and TiO_2/Al_2O_3 ratios and the CIA values along the red soil section are plotted in Fig. 4. The chemical compositions of red soil sediments are characterized by high contents of SiO_2 (71.9% on average), low contents of Al_2O_3 (13.0% on average), Fe_2O_3 (6.0% on average), K_2O (1.6% on average) and TiO_2 (1.1% on average), and minor contents of MgO (0.62% on average), Na_2O (0.27% on average), and CaO (0.24% on average). Trace contents of P_2O_5 (0.06% on average) and MnO (0.04% on average) are also detected (not reported here). Other elements were below the detection limit of XRF. The chemical compositions of Jiujiang red soil sediments show a good agreement with those of Xuancheng red soil sediments (Hong et al., 2009), possibly indicating that the red soil

sediments of Jiujiang and Xuancheng experienced similar pedogenetic processes.

The major differences in chemical composition among the lithological layers are shown by the contents of SiO_2 , Al_2O_3 , and Fe_2O_3 . Considerable variation in contents of SiO_2 , Al_2O_3 , and Fe_2O_3 occurs along the section, and obvious fluctuations are also observed on SiO_2/Al_2O_3 , Al_2O_3/Fe_2O_3 , and SiO_2/Fe_2O_3 ratios. The SiO_2/Al_2O_3 , Al_2O_3/Fe_2O_3 , and SiO_2/Fe_2O_3 ratios show a strong positive correlation with the SiO_2 content, and a relatively weaker correlation with the Al_2O_3 and Fe_2O_3 contents. The Al_2O_3 and Fe_2O_3 contents show a strong positive correlation in the upper section. However, no obvious correlation is observed in the middle and lower sections. A similar trend is found for changes in mobile components K_2O , Na_2O , CaO , and MgO . In comparison to the SiO_2 , Al_2O_3 , and Fe_2O_3 contents, the contents of mobile components K_2O , Na_2O , CaO , and MgO are relatively stable in the middle and lower sections, with relatively higher values in the upper section. The CIA value shows an obviously negative correlation with the K_2O , Na_2O , CaO , and MgO contents, and it is stable in the middle and lower section, with relatively lower values in the upper section. The TiO_2/Al_2O_3 ratio remains relatively constant along the whole section.

3.3. Trace element analysis

The concentrations of Rb, Sr, and the Rb/Sr ratios are plotted in Fig. 5. The content of Rb ranged from 76 to 113 ppm, and the content of Sr ranged from 39 to 88 ppm. The Rb/Sr ratios ranged from 1.22 to 2.17. The concentrations of Rb and Sr are notably higher in the upper section. However, they are relatively lower in the middle and lower sections. The Rb/Sr ratio is lower in the upper section, with notable oscillations relative to the middle and the lower sections, whereas they are relatively stable in the middle and lower sections. Both Rb and Sr concentrations show a strong positive correlation with the contents of the mobile components K_2O , Na_2O , CaO , and MgO , whereas the Rb/Sr ratios show a positive correlation with the CIA values (Figs. 4, 5).

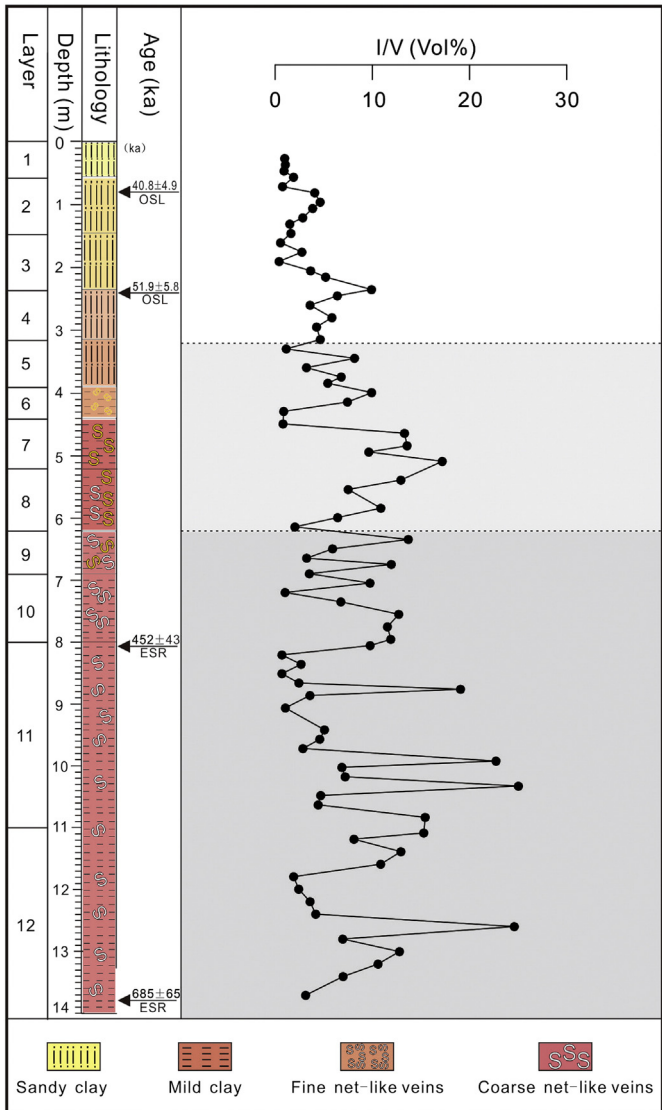


Fig. 3. The content variations of mixed-layer I/V along the Jiujiang red soil section.

4. Discussion

4.1. Mixed-layer illite-vermiculite in the red soil sediments

Vermiculitic mixed-layer clays occur commonly in soils where humid and moderate chemical leaching environments exist, and/or in other sediments persisting through previous weathering cycles (Hong et al., 2014). The weathering of micaceous minerals under temperate climatic conditions can form vermiculitic mixed layers (Bain et al., 1990; Berry and Johns, 1966; Churchman, 1980; McCartan, 1989; Srodon, 1999). In soils the I/V mixed-layer clays are considered to occur as the result of pedogenic processes under temperate-cool conditions leading to the transformation of primary minerals mica and/or illite (Vanderaveroot et al., 1999). The weathering and transformation of 1.0 nm mica and/or illite into I/V have been documented in soils in many areas, such as in the Appalachians (Fagel et al., 1996), Greenland (Petersen and Rasmussen, 1980), New Zealand (Churchman, 1980); the Adirondacks (April et al., 1986), Virginia (McCartan, 1989), Scotland (Bain et al., 1990), and the Southern Taiga (Bonifacio et al., 2009).

Mixed-layer I/V clays are characterized by basal XRD peaks between 1.0 nm and 1.4 nm for air-dried, Mg-saturated, and glycol-solvated samples, whereas the 001 spacing of the vermiculite layers in mixed-layered I/V would change from 1.4 nm to 1.0 nm on heating, indicating the loss

of water and hydroxy-cations from their interlayers. The XRD results showed that mixed-layer I/V is widely distributed in the whole section (Fig. 2A–C). The middle and lower portions of the red soil section contained mainly mixed-layer I/V with vermiculite layers (Fig. 3B–C), whereas the upper portion, by contrast, contained mainly mixed-layer I/V with hydroxy-interlayered vermiculite layers (Fig. 2A). Different vermiculitic layers in mixed-layer I/V might suggest different pedogenic processes during their formation (Fig. 6).

HRTEM lattice fringe images clearly indicate randomly mixed-layer I/V with straight 1.0 nm illite layers interstratified with 1.4 and/or 1.2 nm vermiculite layers that occur within I/V crystals (Yin et al., 2013). The 1.4 nm spacing corresponds to hydrated phases with two sheets of water molecules in the interlayer region, while the 1.2 nm spacing corresponds to hydrated phases with only a single sheet of water molecules (Vali and Hesse, 1992; Walker, 1975). The 1.4 nm and 1.2 nm spacing fringes are straight or corrugated and are interstratified with 1.0 nm fringes, suggesting that the vermiculitic clays in Jiujiang resulted from the weathering of illite in the Jiujiang soil sediments (Hong et al., 2014). The illite to vermiculite transition process might involve an exchange of K^+ by hydrated cations or hydroxyl interlayers associated with a swelling of the illite (Barnhisel and Bertsch, 1989; Meunier, 2007; Velde and Meunier, 2008).

XRD analysis showed that mixed-layer I/V occurred commonly along the whole Jiujiang section, in association with illite, kaolinite, and vermiculite or hydroxyl-interlayered vermiculite (Fig. 2A–C). Mixed-layer I/V deriving from the weathering of illite was clearly revealed by HRTEM lattice fringe images (Yin et al., 2013), and it has a notably higher content in the middle and lower portions compared to that of the upper portion (Fig. 3). In southern China, red soil sediments from the mid-lower reaches of the Yangtze River were generally considered to have an aeolian origin with synchronous pedogenesis (Hu et al., 2010; Xiong et al., 2002). Recent geochemical and isotopic composition studies suggest that the red soil sediments are in fact derived from the drainage basins of the mid-lower reaches of the Yangtze River with intense chemical weathering (Hao et al., 2010; Hong et al., 2013a, 2013b). During the deposition-pedogenesis process, the inherited clay minerals would transform to the stable types through chemical weathering, in correspondence with the climatic conditions (Hong et al., 2014; Yin et al., 2013). Generally, illite layers altered into vermiculite layers by losing K and gaining hydrated exchangeable cations during the moderate chemical weathering process. Thus, a mixed-layer I/V mineral would be formed as an intermediate in the illite to vermiculite transition (Bonifacio et al., 2009; Churchman, 1980; Vanderaveroot, 1996). The red soil sediments in mid-lower reaches of the Yangtze River experienced syndepositional pedogenesis with an additional pedogenic process (Hong et al., 2010), and this special pedogenic environment could lead to an incomplete transformation of illite to vermiculite and favor the formation of metastable intermediates of I/V minerals (Hong et al., 2014). In Pleistocene sediments of the northwestern Atlantic Ocean, mixed-layer I/V is much more abundant during interglacial periods than during glacial ones (Vanderaveroot et al., 2000), which indicates that its occurrence and abundance can be used as an effective paleoclimate proxy in the red soil sediments. The contents of mixed-layer I/V oscillate along the Jiujiang section and show a decreasing trend upwards towards the surface, suggesting decreased weathering since the middle Pliocene.

4.2. Chemical weathering intensity of the Jiujiang red soil sediments

The CIA values of the Jiujiang red soil sediments range from 74.8 to 88.6, which are much larger values than those of 50 to 75 for loess deposits (Gallet et al., 1998; Yin et al., 2012). However, they are very close to the values of 85.6 to 90.2 for the Xuancheng red soil sediments (Hong et al., 2009). The larger CIA values from Jiujiang and Xuancheng sections indicate that the red soil sediments from southern China have experienced more intense chemical weathering than the loess deposits

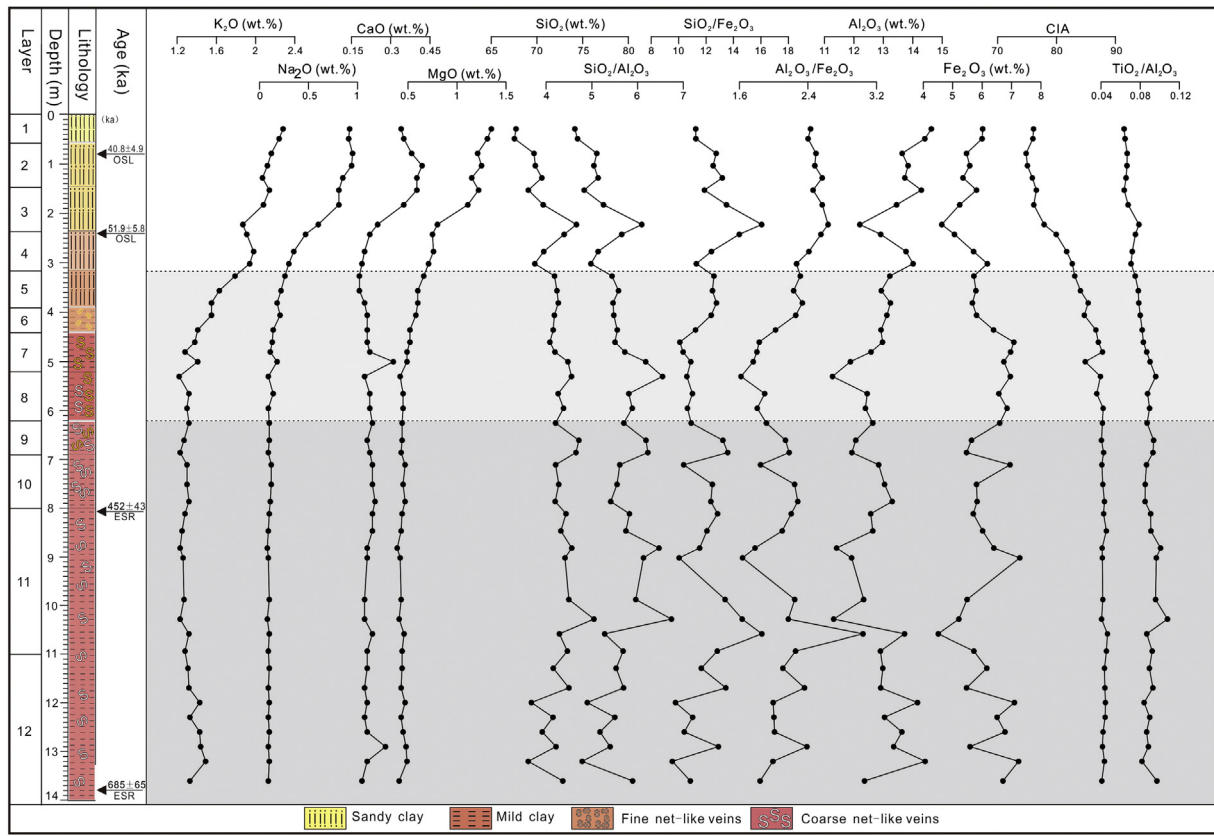


Fig. 4. Major elements and chemical indices of the Jiujiang red soil sediments.

from northern China. Furthermore, the CIA values in the middle (85.9 in average) and lower portions (88.1 in average) are higher than those of the upper portion (77.5 in average). The upward decreasing trend in CIA average values suggests decreased weathering towards the surface of the section. A similar trend of changes in CIA values was also found in the Xuancheng section (Hong et al., 2009; Xiong et al., 2000). Generally, CIA values range from 60 to 80, indicating a moderate degree of pedogenesis, whereas a range from 80 to 100 indicates intense pedogenesis (Dal'Bó et al., 2010; Qiao et al., 2011; Sheldon et al., 2002). Therefore, the characteristic CIA values in the Jiujiang red soil sediments represent a moderate weathering of the upper portion and an intense weathering of the middle and lower portions during pedogenesis.

The elemental distribution within the soil profile is a sensitive index for measuring the intensity of chemical weathering and can be used for assessing the nature and degree of weathering (Nesbitt and Young, 1984). The leaching of soluble components in the weathering profile leads to an increase in the concentrations of relatively insoluble species (Brimhall and Dietrich, 1987). The chemical composition of the Jiujiang red soil sediments indicate a preferential leaching of K₂O, Na₂O, CaO, and MgO and an enrichment of SiO₂, Al₂O₃, and Fe₂O₃ under the intensive chemical weathering (Fig. 4). The mobile components K₂O, Na₂O, CaO, and MgO exhibit a generally upward decrease within the red soil section, with intense fluctuations in the upper portion. The upward increasing trend of the mobile components also reflects a decreased weathering, in good agreement with the result of CIA values. However, the major components SiO₂, Al₂O₃, and Fe₂O₃ and the SiO₂/Al₂O₃, Al₂O₃/Fe₂O₃, and SiO₂/Fe₂O₃ ratios show notable fluctuations along the section. The fluctuations of SiO₂/Fe₂O₃ and Al₂O₃/Fe₂O₃ indicate that degrees of weathering of the soil horizons alternate along the section, suggesting intense climatic oscillations have occurred in the area since the middle Pleistocene. However, no obvious decreasing or increasing

trend was observed in the plots of the major components SiO₂, Al₂O₃, and Fe₂O₃ and the SiO₂/Al₂O₃, Al₂O₃/Fe₂O₃, and SiO₂/Fe₂O₃ ratios.

The Rb/Sr ratios in the Jiujiang section exhibit a similar decreasing trend upwards to the CIA values, with slight fluctuations in the middle and lower portions. This also suggests decreased weathering towards the surface. The relatively higher Rb/Sr ratios in the middle portion (1.99 on average) and lower portion (2.01 on average) in contrast to Rb/Sr ratio in the upper portion (1.46 on average) suggest a more intense weathering prevailing during their pedogenesis. The upward decreasing weathering revealed by the Rb/Sr ratios and the CIA values is also very consistent with the result uncovered by mixed-layer I/V content changes.

4.3. Paleoclimatic evolution in the Jiujiang area

The middle and lower portions are mainly net-like red soil sediments. The net-like soils in southern China formed under extremely warm humid conditions were under the control of summer monsoons, resulting in the depletion of Fe oxides from the white veins and the accumulation of Fe oxides in the red matrix (Yin and Guo, 2006). Therefore, the striking difference between the red matrix and the white veins is shown by the relative content of Fe oxides. The particle size analysis indicates that the white veins and the red matrix of the net-like soils might have the same origin (Hong et al., 2010). Under seasonally warm and humid climatic conditions, climate changes will cause frequent rising and falling of the groundwater table, whereas a seasonally dry and wet environment may cause frequent swelling and shrinking and development of fissures in the soils. The occurrence of fissures would promote the dissolution and leaching of Fe oxides and finally would create the white net-like veins near fissures and the red matrix away from fissures (Hong et al., 2010). Red soil sediments in the upper portion displayed a homogeneous structure and are in

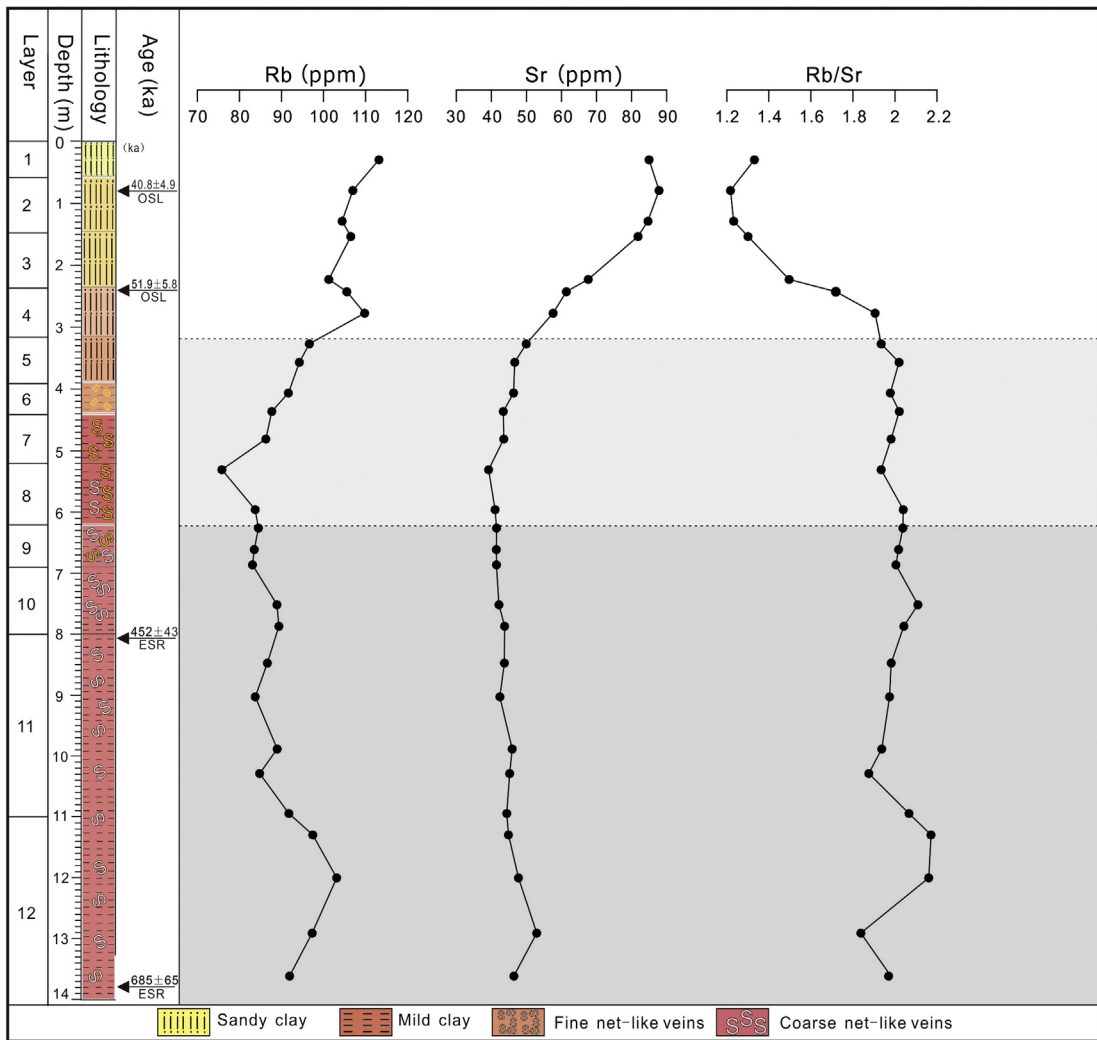


Fig. 5. Trace elements and Rb/Sr ratios of the Jiujiang red soil sediments.

chronological agreement with the deposition of the Xiashu loess (Liu, 1985); they were probably influenced by an intensification of the winter monsoon as in the case of the Xiashu loess. The climate oscillated between warm and cool conditions in the Pleistocene era and resulted in the alternation of mainly soil-forming and loess-forming stages in northern China to central Asia (Liu, 1985; Perederij, 2001). The red soil sediments in the middle to lower reaches of the Yangtze River in southern China have also reflected a similar climate evolution pattern that is embedded in Quaternary sediments in northern China (Hong et al., 2010; Zhao and Yang, 1995). The climate oscillations between warm and cool conditions will result in different amounts of mixed-layer I/V, CIA values, and Rb/Sr ratios in the red soil sediments. In other words, the variations of the mixed-layer I/V contents, CIA values, and Rb/Sr ratios along the red soil section could provide a great opportunity to decipher climate evolution since the Pleistocene.

As reflected by the mixed-layer I/V contents in combination with CIA values and Rb/Sr ratios of the soil sediments, an upward decreasing weathering trend was revealed along the Jiujiang section, resulting from a response to the regional climate. An upward decreasing weathering indicates drier and cooler climates over the soil-forming process in the upper portion relative to the middle and lower portions. The middle to lower portions of the Jiujiang section had an apparent net-like structure, with notably wider and longer white veins in the lower portion and relatively thin and short ones in the middle portion. Higher mixed-layer I/V contents, CIA values, and Rb/Sr ratios in the lower portion than those in the middle portion suggest that warmer

and more humid climates prevailed in the lower portion during pedogenesis. Formation of the white net-like veins in the soil profiles needed abundant rainfall with clear dry seasons (Hong et al., 2010; Yin and Guo, 2006), and the well-developed net-like veins in the lower portions are indicative of warmer and more humid climates over the soil-forming process relative to the middle portion, in good agreement with more abundant mixed-layer I/V clays, as well as the higher CIA values and Rb/Sr ratios of the lower portion. Hence, the upward decreasing trend of the mixed-layer I/V contents, CIA values, and Rb/Sr ratios within the Jiujiang section reveal a gradual climate change from most warm and humid to relatively cool and dry from the Middle Pleistocene to the Late Pleistocene. The climate evolution revealed by the mixed-layer I/V contents, CIA values, and Rb/Sr ratios of the Jiujiang red soil sediments is very consistent with that documented in hematite/goethite ratios and magnetic properties of European loess-paleosol sequences (Buggle et al., 2014). This also indicates that the climate change since the mid-Pleistocene was a global event and the red soil sequences in southern China could probably be used to test the response of tropical to subtropical regions to global climate changes.

4.4. Paleoclimate cycles documented in the red soil sediments

In northern China, the loess-paleosol sequence has become an effective terrestrial proxy revealing the multiple cyclic changes of Quaternary climates, which is very consistent with the marine oxygen-isotopic record (An et al., 1991; Chen et al., 1999; Deng et al., 2006;

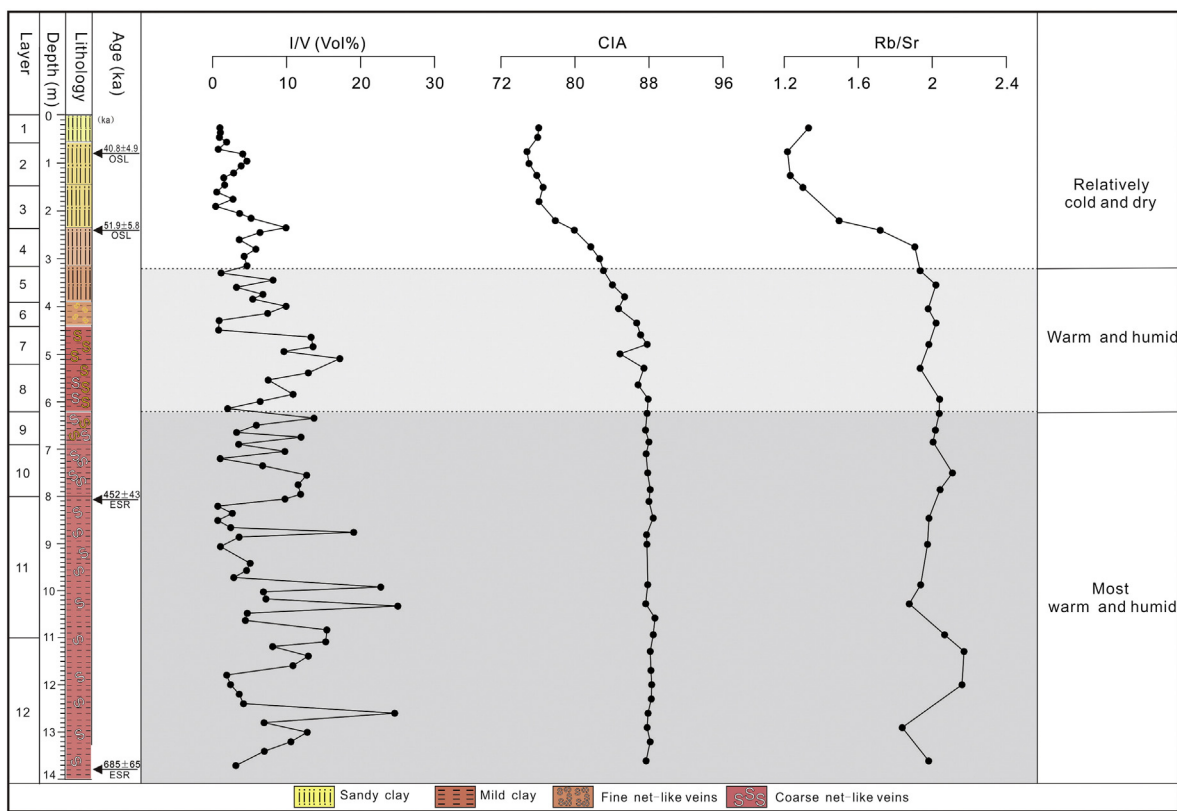


Fig. 6. An upward decreasing weathering trend along the Jiujiang red soil section.

Liu, 1985; Xiao et al., 1995). In southern China, Quaternary red soil sediments are distributed extensively. A typical Quaternary red soil section is often composed of a yellow-brown-colored layer (YBE), a uniform red-colored layer (URC), and a net-like or reticulate red layer (RRC) from top to bottom (Gong, 1985; Hu et al., 2015). Based on the evidence from grain size and geochemistry of the red soil sediments, there was no depositional break from YBE to URC to RRC (Hu et al., 2015). Quaternary red soil sediments in southern China were believed by many researchers to document the same multiple climate cycles as the loess-paleosol sequence (Li et al., 1998; Yang et al., 1991; Yang et al., 1995). Based on the sedimentary characteristics and grain-size distribution, multiple dust deposit-pedogenesis cycles has been revealed in Xiangyang red soil sediments from Anhui province which could be compared with the loess-paleosol sequence in the Chinese Loess Plateau (Yang et al., 1991). Magnetic susceptibility, stable carbon isotopic compositions, and geochemical studies came to a similar conclusion that several deposit-pedogenesis cycles existed in the Xiangyang red soil section (Hu et al., 2003; Li et al., 1998; Yang et al., 1995). The pedogenesis is closely related to climatic conditions; therefore, deposit-pedogenesis cycles documented in red soil reflect climatic cycles related to the glacial and interglacial. However, after detailed investigation on Xiangyang red soil sediments, Hu et al. (2003) proposed that the evidences for deposit-pedogenesis cycles related to paleoclimatic changes were not sufficient to indicate climate changes. They found that the magnetic parameters such as χ , SIRM, and χ_{ARM} showed higher values in slightly weathered red soil layers and lower values in intensely weathered red soil layers, whereas these parameters presented the opposite changes in slightly weathered layers and intensely weathered layers of a loess-paleosol sequence (An et al., 1991; Hao et al., 2008; Jordanova et al., 2007; Kukla et al., 1990; Zhou et al., 1990). Therefore, they considered that the magnetic parameters, which are quite effective on the loess-paleosol sequence in northern China, were inappropriate for the red soil sediments due to the destruction or leaching of ferromagnetic minerals related to more intense weathering in southern

China. They also suggested that other indices such as the hues and organic $\delta^{13}\text{C}$ characteristic of the red soil sediments cannot prove the existence of multiple deposit-pedogenesis cycles in the Xiangyang section (Hu et al., 2003). Hence, whether multiple deposit-pedogenesis cycles related to paleoclimatic changes exist in the red soil sediments is still controversial.

In the Jiujiang red soil section, the variations in contents of mixed-layer I/V show a strong positive correlation with the changes in magnetic susceptibility of loess-paleosol sediments (Fig. 7). Their synchronous variation indicates that southern China and northern China experienced a similar climate change from the mid-Pleistocene to the late Pleistocene. The higher values of the content of mixed-layer I/V and the magnetic susceptibility indicate a warm and humid climate, which correlates well with higher values of marine oxygen isotopic values for the same stages (Fig. 7), indicating that multiple sub-climate cycles related to the deposit-pedogenesis process existed in the red soil sediments of southern China. This also suggests that sub-climatic events were of a global scale since the mid-Pleistocene. The obvious fluctuations of $\text{SiO}_2/\text{Al}_2\text{O}_3$, $\text{Al}_2\text{O}_3/\text{Fe}_2\text{O}_3$, and $\text{SiO}_2/\text{Fe}_2\text{O}_3$ also suggest that multiple climate cycles occurred in the area during the Pleistocene (Fig. 4). However, multiple sub-climate cycles cannot be identified within CIA values. Quaternary red soil sediments are extensively distributed in southern China, and were formed under long-term humid and warm climates and were intensively weathered (Gong, 1985; Xi, 1965). The much higher CIA average values also indicate that the Jiujiang red soil sediments were generally intensively weathered compared with loess-paleosol sediments (Gallet et al., 1998; Yin et al., 2012). Due to the strong leaching and migration of elements caused by the intense chemical weathering, the mobile components K_2O , Na_2O , CaO , and MgO in red soil sediments are more depleted compared with those of loess-paleosol sediments in southern China (Yin et al., 2012). In other words, the total contents of the mobile components are too low for Al_2O_3 contents in the red soil sediments, resulting in no

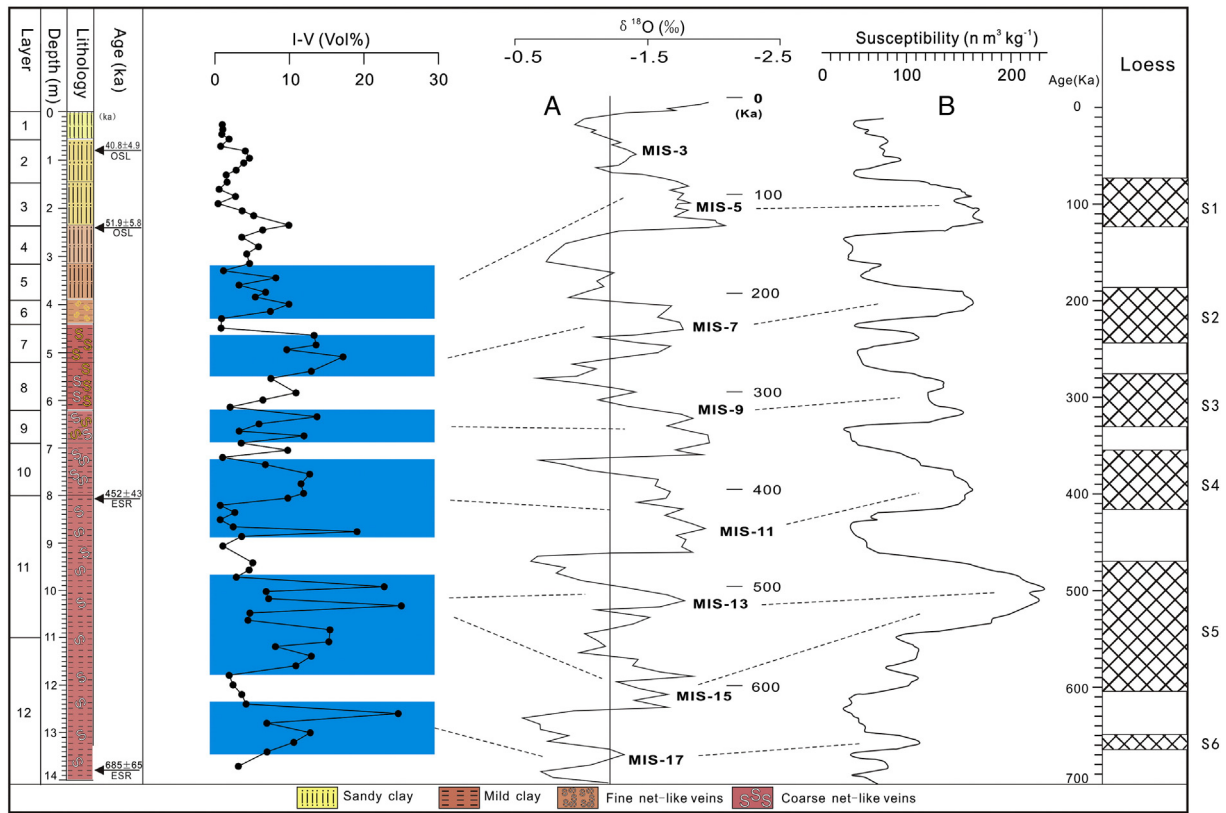


Fig. 7. Comparison of the variation of mixed-layer I/V content and magnetic susceptibility of loess-paleosol sequence with marine oxygen isotope. a. $\delta^{18}\text{O}$ records of the equatorial Pacific Core V28-238 adapted from Shackleton and Opdyke (1973); b. magnetic susceptibility record of the Chinese loess obtained by averaging data from localities Luochuan and Xifeng (Kukla et al., 1990).

obvious oscillations on CIA curves. Although the general climate evolution can be uncovered by CIA values, sub-climatic events cannot be identified by them in the Jiujiang red soil sediments. This also suggests that CIA values are not suitable for revealing the sub-climatic cycles in intensively weathered sediments.

The representative bulk samples were investigated to detect non-clay minerals by XRD, and the XRD results show that non-clay minerals quartz, orthoclase, and plagioclase were identified using 0.425 nm, 0.324 nm and 0.319 nm reflections, respectively (Fig. 8A–C). The absence of other silicates except orthoclase and plagioclase also suggests an intense weathering condition predominating since the mid-Pleistocene. The intense weathering of silicates resulted in a great depletion of Sr and relative enrichment of Rb in the red soil sediments, leading to generally higher Rb/Sr ratios than those of loess–paleosol sediments (Chen et al., 1999). Slight fluctuations in Rb/Sr ratios also suggest sub-climatic cycles during the Pleistocene age. However, it is very difficult to correlate Rb/Sr ratios with marine oxygen isotopic stages because they fluctuate only slightly. Net-like red soil sediments are widely developed in the middle to lower portions of the Jiujiang section. Many researchers believe that white veins in the net-like red soil were formed by leaching the fissures in the homogenous parent red matrix, finally resulting in the depletion of Fe_2O_3 in the white veins and the accumulation of Fe_2O_3 in the red matrix. Conversely, SiO_2 and Al_2O_3 were found to be enriched in the white veins and depleted in the red matrix (Hong et al., 2010; Lai et al., 2005; Li and Gu, 1997; Yin and Guo, 2006). The leaching under seasonally warm and humid climatic conditions led to the inhomogeneous distribution of SiO_2 , Al_2O_3 , and Fe_2O_3 in the white veins and the red matrix. Therefore, the obvious fluctuations of $\text{SiO}_2/\text{Al}_2\text{O}_3$, $\text{Al}_2\text{O}_3/\text{Fe}_2\text{O}_3$, and $\text{SiO}_2/\text{Fe}_2\text{O}_3$ indicating multiple climate cycles in the net-like red soil sediments might be derived from non-uniform sampling. However, the clay assemblage in the white veins and the

red matrix are quite similar (Hong et al., 2010; Yin and Guo, 2006). That is, mixed-layer I/V has the same content in the white veins and the red matrix of the same soil layer. Hence, the mixed-layer I/V contents can be effectively used to document the climatic information during the formation of the net-like red soil sediments. It has been also proven to be an effective paleoclimate proxy for northwestern Atlantic Pleistocene sediments (Vanderaverde et al., 2000).

Red soil sediments in southern China were subjected to relatively intense weathering and pedogenic alteration under long-term warm and humid conditions, resulting in the transformation of magnetic minerals and the strong leaching and migration of elements, as well as the lack of fossils in the red soil sediments (Gong, 1985; Hong et al., 2012). Therefore, the geochemistry and paleontology are greatly limited for revealing the climatic information documented in the red soil sediments. In particular, magnetostratigraphy, widely used in the study of the loess–paleosol sediments in northern China, is no longer suitable for the red soil sediments in southern China (Hu et al., 2009; Yang et al., 2008). Therefore, it is difficult to reveal the same multiple climate cycles related to deposit-pedogenesis processes as shown by the loess–paleosol sequence. The mixed-layer I/V contents, CIA values, and Rb/Sr ratios of the Jiujiang soil sediments jointly revealed that the paleoclimate transformed from warm/humid to cool/dry from the Middle Pleistocene to the Late Pleistocene, quite consistent with the climatic information documented in other Quaternary sediments (Buggle et al., 2014; Hong et al., 2013a, 2013b; Hu et al., 2015; Kostić and Protić, 2000; Marković et al., 2009). However, the warm/humid to cold/dry transition is not reflected by the $\text{SiO}_2/\text{Al}_2\text{O}_3$, $\text{Al}_2\text{O}_3/\text{Fe}_2\text{O}_3$, and $\text{SiO}_2/\text{Fe}_2\text{O}_3$ ratios. Among those indices, the mixed-layer I/V contents can not only uncover the whole climate trend documented in the red soil sediments since the Middle Pleistocene, but can also reveal the sub-climate cycles related to deposit-pedogenesis processes.

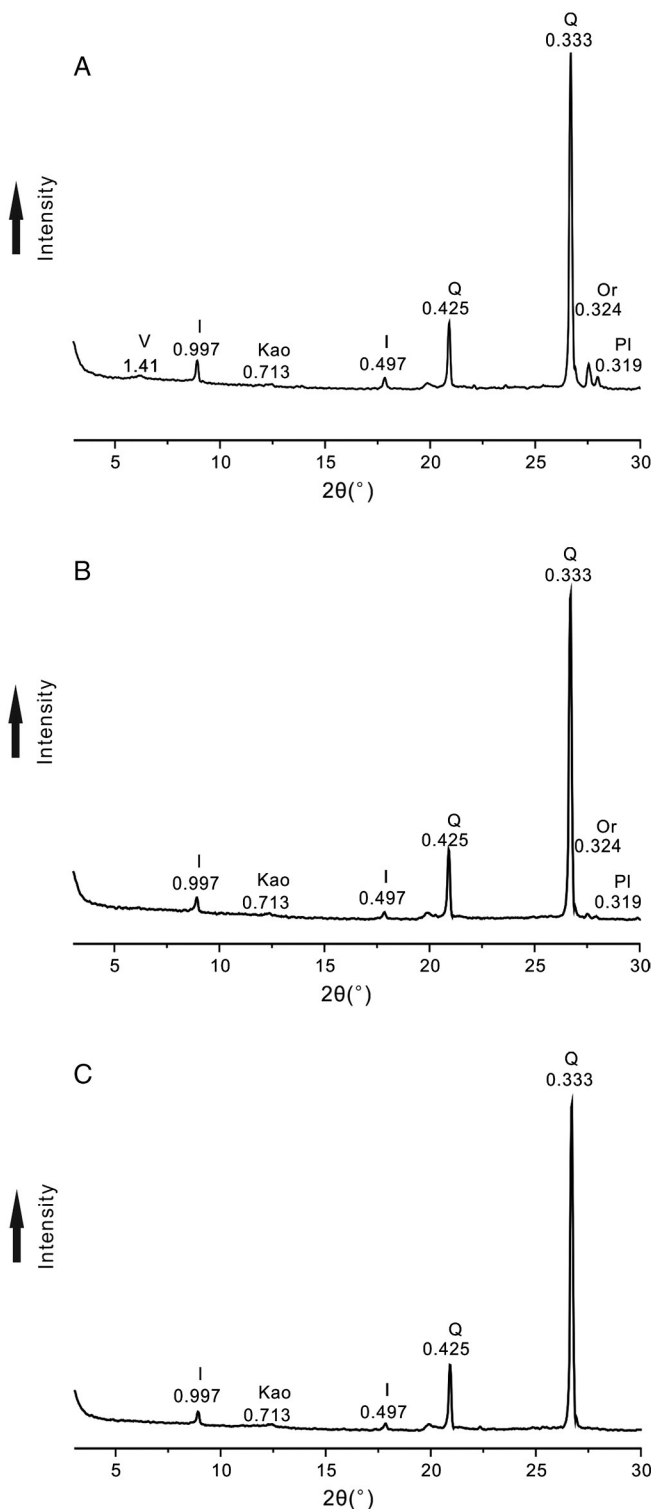


Fig. 8. Representative XRD patterns of bulk samples (A, B, and C correspond to representative samples from the upper, the middle, and the lower portions of the Jiujiang red soil sediments, respectively). V-vermiculite; I-illite; Kao-kaolinite; Q-quartz; Or-orthoclase; PI-plagioclase.

5. Conclusions

XRD analysis suggests that mixed-layer I/V was ubiquitous in all the soil layers of the Jiujiang red soil sediments, with its content fluctuating within the soil section. In the XRD patterns, mixed-layer I/V was identified by the basal peaks ranging from 1.0 to 1.4 nm for Mg-saturated samples, whose spacings did not alter after glycol treatment. Its 001

spacing would collapse to 1.0 nm with temperature, owing to the loss of water and hydroxyl in its interlayer. The upward decrease of the mixed-layer I/V contents reveal a gradual climate change from warmest and most humid to warm and humid to relatively cool and dry from the Middle Pleistocene to the Late Pleistocene. The content variations of mixed-layer I/V show a strong positive correlation with the changes of magnetic susceptibility of loess-paleosol sediments and the higher values of its content correlate well with higher values of magnetic susceptibility in the loess-paleosol sediments and marine oxygen isotopic stages of higher values. This suggests multiple sub-climate cycles related to deposit-pedogenesis process occurred in red soil sediments of southern China.

The CIA values and Rb/Sr ratios in the Jiujiang red soil sediments show the same upward decreasing trend to the mixed-layer I/V contents, jointly revealing the climate shift from warm/humid to cool/dry since the Middle Pleistocene. No obvious oscillations were observed on the curve of CIA values and Rb/Sr ratios, suggesting that multiple sub-climate cycles cannot be identified by them. Although, the $\text{SiO}_2/\text{Al}_2\text{O}_3$, $\text{Al}_2\text{O}_3/\text{Fe}_2\text{O}_3$, and $\text{SiO}_2/\text{Fe}_2\text{O}_3$ ratios show notable fluctuations along the section, no obvious decreasing or increasing trend was observed. The leaching under seasonally warm and humid climatic conditions led to inhomogeneous distribution of SiO_2 , Al_2O_3 , and Fe_2O_3 in the white veins and the red matrix, suggesting that the obvious fluctuations of $\text{SiO}_2/\text{Al}_2\text{O}_3$, $\text{Al}_2\text{O}_3/\text{Fe}_2\text{O}_3$, and $\text{SiO}_2/\text{Fe}_2\text{O}_3$ indicating multiple climate cycles in the net-like red soil sediments might be derived from non-uniform sampling. Among those indices, the mixed-layer I/V contents can not only reveal the whole climate trend reflected in the red soil sediments since the Middle Pleistocene, but can also delineate the sub-climate cycles related to deposit-pedogenesis processes. Red soil sediments in southern China were subject to relatively intense weathering and pedogenic alteration under long-term warm and humid conditions. However, many climatic indicators evident in the loess-paleosol sediments in northern China are not suitable for the red soil sediments in southern China.

Acknowledgments

This work was supported by the Natural Science Foundation of China (41402036, 41472041 and 41272053) and China Postdoctoral Science Foundation (2014M562084). The authors wish to thank Dr. Y. S. Gu for the sample preparation, and Yu J. S. for the XRD analyses. We thank Dr. Christopher Bae (editor) and two anonymous reviewers for their incisive reviews of the manuscript.

References

- Allen, B.L., Hajek, B.F., 1989. Mineral occurrence in soil environments. In: Dixon, J.B., Weed, S.B. (Eds.), *Minerals in Soil Environments*. Soil Science Society of America, pp. 199–278.
- An, Z., Kukla, G.J., Porter, S.C., Xiao, J., 1991. Magnetic susceptibility evidence of monsoon variation on the Loess Plateau of central China during the last 130,000 years. *Quat. Res.* 36 (1), 29–36.
- April, R.H., Hluchy, M.M., Newton, R.M., 1986. The nature of vermiculite in Adirondack soils and till. *Clay Clay Miner.* 34 (5), 549–556.
- Bain, D.C., Mellor, A., Wilson, M.J., 1990. Nature and origin of an aluminous vermiculitic weathering product in acid soils from upland catchments in Scotland. *Clay Miner.* 25 (4), 467–475.
- Barnhisel, R.I., Bertsch, P.M., 1989. Chlorites and hydroxyl-interlayered vermiculite and smectite. In: Dixon, J.B., Weed, S.B. (Eds.), *Minerals in Soil Environments*. Soil Science Society of America, Madison, WI, pp. 728–788.
- Berry, R.W., Johns, W., 1966. Mineralogy of the clay-size fractions of some North Atlantic Arctic Ocean bottom current. *Geol. Soc. Am. Bull.* 77 (2), 183–196.
- Bertsch, P.M., Thomas, G.W., 1985. Potassium status of temperate region soils. In: Robert, D.M. (Ed.), *Potassium in Agriculture*. American Society of Agronomy, Crop Science Society of America & Soil Science Society of America, Madison, Wisconsin, pp. 201–276.
- Bonifacio, E., Falsone, G., Simonov, G., Sokolova, T., Tolpeshka, I., 2009. Pedogenic processes and clay transformations in bisequeal soils of the Southern Taiga zone. *Geoderma* 149 (1), 66–75.
- Brimhall, G.H., Dietrich, W.E., 1987. Constitutive mass balance relations between chemical composition, volume, density, porosity, and strain in metasomatic hydrochemical systems: results on weathering and pedogenesis. *Geochim. Cosmochim. Acta* 51 (3), 567–587.

Brown, G., Brindley, G.W., 1980. X-ray diffraction procedures for clay mineral identification. In: Brindley, G.W., Brown, G. (Eds.), *Crystal Structures of Clay Minerals and Their X-ray Identification*. Mineralogical Society, London, pp. 305–359.

Bugge, B., Hambach, U., Müller, K., Zöller, L., Marković, S.B., Glaser, B., 2014. Iron mineralogical proxies and Quaternary climate change in SE-European loess-paleosol sequences. *Catena* 117, 4–22.

Catt, J.A., 1991. Soils as indicators of Quaternary climatic change in mid-latitude regions. *Geoderma* 51 (1), 167–187.

Chen, J., An, Z., Head, J., 1999. Variation of Rb/Sr ratios in the Loess-Paleosol sequences of central China during the last 130,000 years and their implications for monsoon paleoclimatology. *Quat. Res.* 51 (3), 215–219.

Chen, Y., Li, X., Han, Z., Yang, S., Wang, Y., Yang, D., 2008. Chemical weathering intensity and element migration features of the Xiaoshu loess profile in Zhenjiang, Jiangsu Province. *J. Geogr. Sci.* 18 (3), 341–352.

Churchman, G.J., 1980. Clay minerals formed from micas and chlorites in some New Zealand soils. *Clay Miner.* 15, 59–76.

Churchman, G.J., Lowe, D.J., 2012. Alteration, formation and occurrence of minerals in soils. In: Huang, P.M., Li, Y., Sumner, M.E. (Eds.), *Handbook of Soil Sciences, 2nd Edition. Properties and Processes*. CRC Press, Boca Raton, Florida, pp. 20.1–20.72.

Dal'Bó, P.F.F., Basílico, G., Angelica, R.S., 2010. Factors of paleosol formation in a Late Cretaceous eolian sand sheet paleoenvironment, Marília Formation, Southeastern Brazil. *Palaeogeogr. Palaeoclimatol. Palaeoecol.* 292 (2), 349–365.

Deng, C., Shaw, J., Liu, Q., Pan, Y., Zhu, R., 2006. Mineral magnetic variation of the Jingbian loess/paleosol sequence in the northern Loess Plateau of China: implications for Quaternary development of Asian aridification and cooling. *Earth Planet. Sci. Lett.* 241 (1), 248–259.

Du, X., Xie, X., Lu, Y., Ren, J., Zhang, S., Lang, P., Cheng, T., Su, M., Zhang, C., 2011. Distribution of continental red paleosols and their forming mechanisms in the Late Cretaceous Yaojia Formation of the Songliao Basin, NE China. *Cretac. Res.* 32 (2), 244–257.

Fagel, N., Robert, C., Hillaire-Marcel, C., 1996. Clay mineral signature of the NW Atlantic boundary undercurrent. *Mar. Geol.* 130 (1–2), 19–28.

Gallet, S., Jahn, B., Van Vliet Lanoë, B., Dia, A., Rossello, E., 1998. Loess geochemistry and its implications for particle origin and composition of the upper continental crust. *Earth Planet. Sci. Lett.* 156 (3), 157–172.

Gong, Z.T., 1985. Bio-geochemistry of the red weathering crusts. In: Li, Q.K. (Ed.), *Red Soils in China*. Science Press, Beijing, pp. 24–40 (in Chinese).

Hao, Q., Oldfield, F., Bloemendal, J., Guo, Z., 2008. The magnetic properties of loess and paleosol samples from the Chinese Loess Plateau spanning the last 22 million years. *Palaeogeogr. Palaeoclimatol. Palaeoecol.* 260 (3), 389–404.

Hao, Q., Guo, Z., Qiao, Y., Xu, B., Oldfield, F., 2010. Geochemical evidence for the provenance of middle Pleistocene loess deposits in southern China. *Quat. Sci. Rev.* 29 (23–24), 3317–3326.

Harris, W., White, G.N., 2008. X-ray diffraction techniques for soil mineral identification. In: Ulery, A.L., Drees, R. (Eds.), *Methods of Soil Analysis. Part 5. Mineralogical Methods*. Soil Science Society of America Book Series, Madison.

Hong, H., Li, Z., Xue, H., Zhu, Y., Zhang, K., Xiang, S., 2007. Oligocene clay mineralogy of the Linxia Basin: evidence of Paleoclimatic evolution subsequent to the initial-stage uplift of the Tibetan Plateau. *Clay Clay Miner.* 55 (5), 491–503.

Hong, H., Gu, Y., Li, R., Zhang, K., Li, Z., 2009. Clay mineralogy and geochemistry and their palaeoclimatic interpretation of the Pleistocene deposits in the Xuancheng section, southern China. *J. Quat. Sci.* 25 (5), 662–674.

Hong, H., Gu, Y., Yin, K., Zhang, K., Li, Z., 2010. Red soils with white net-like veins and their climate significance in south China. *Geoderma* 160 (2), 197–207.

Hong, H., Du, D., Li, B., Churchman, G.J., Yin, K., 2012. Mixed-layer clay minerals in the Xuancheng red clay sediments, Xuancheng, Anhui Province. *Earth Sci. J. China Univ. Geosci.* 37 (3), 424–432 (in Chinese with English abstracts).

Hong, H., Wang, C., Zeng, K., Gu, Y., Wu, Y., Yin, K., Li, Z., 2013a. Geochemical constraints on provenance of the mid-Pleistocene red earth sediments in subtropical China. *Sediment. Geol.* 290, 97–108.

Hong, H., Gu, Y., Yin, K., Wang, C., Li, Z., 2013b. Clay record of climate change since the mid-Pleistocene in Jiujiang, south China. *Boreas* 42 (1), 173–183.

Hong, H., Churchman, G.J., Yin, K., Li, R., Li, Z., 2014. Randomly interstratified illite-vermiculite from weathering of illite in red earth sediments in Xuancheng, southeastern China. *Geoderma* 214, 42–49.

Hu, X., Cheng, T., Wu, H., 2003. Do multiple cycles of aeolian deposit-pedogenesis exist in the reticulate red clay sections in southern China? *Chin. Sci. Bull.* 48 (12), 1251–1258.

Hu, X., Zhu, Y., Shen, M., 2005. Grain-size evidence for multiple origins of the reticulate red clay in southern China. *Chin. Sci. Bull.* 50 (9), 910–918.

Hu, X., Wei, J., Xu, L., Zhang, G., Zhang, W., 2009. Magnetic susceptibility of the Quaternary Red Clay in subtropical China and its paleoenvironmental implications. *Palaeogeogr. Palaeoclimatol. Palaeoecol.* 279 (3–4), 216–232.

Hu, X.F., Wei, J., Du, Y., Xu, L.F., Wang, H.B., Zhang, G.L., Ye, W., Zhu, L.D., 2010. Regional distribution of the Quaternary Red Clay with aeolian dust characteristics in subtropical China and its paleoclimatic implications. *Geoderma* 159, 314–317.

Hu, X., Du, Y., Liu, X., Zhang, G., Jiang, Y., Xue, Y., 2015. Polypedogenic case of loess overlying red clay as a response to the Last Glacial–Interglacial cycle in mid-subtropical Southeast China. *Aeolian Res.* 16, 125–142.

Ismail, F.T., 1970. Biotite weathering and clay formation in arid and humid regions, California. *Soil Sci.* 109 (4), 257–261.

Ji, H., Wang, S., Ouyang, Z., Zhang, S., Sun, C., Liu, X., Zhou, D., 2004. Geochemistry of red residua underlying dolomites in karst terrains of Yunnan–Guizhou Plateau: I. The formation of the Pingba profile. *Chem. Geol.* 203 (1–2), 1–27.

Jordanova, D., Hus, J., Geeraerts, R., 2007. Palaeoclimatic implications of the magnetic record from loess/paleosol sequence Viatovo (NE Bulgaria). *Geophys. J. Int.* 171 (3), 1036–1047.

Kemp, R.A., Derbyshire, E., 1998. The loess soils of China as records of climatic change. *Eur. J. Soil Sci.* 49 (4), 525–539.

Kostić, N., Protić, N., 2000. Pedology and mineralogy of loess profiles at Kapela-Batajnica and Stalac, Serbia. *Catena* 41 (1), 217–227.

Kovács, J., 2007. Chemical weathering intensity of the Late Cenozoic “Red Clay” deposits in the Carpathian Basin. *Geochem. Int.* 45 (10), 1056–1063.

Kukla, G., 1987. Loess stratigraphy in central China. *Quat. Sci. Rev.* 6 (3), 191–219.

Kukla, G., An, Z.S., Melice, J., 1990. Magnetic susceptibility record of Chinese loess. *Trans. R. Soc. Edinb. Earth Sci.* 81 (4), 263–288.

Lai, H.Z., Mo, D.W., Li, X.P., 2005. Genesis of reticulate clay in the laterite of the Dongting Basin. *Acta Sci. Nat. Univ. Pekin.* 41 (2), 240–248 (in Chinese with English abstracts).

Li, C., Gu, Y., 1997. Stratigraphic study on the vermicular red earth at Xiushui County, Jiangxi Province. *J. Stratigr.* 21 (3), 226–232 (in Chinese with English abstracts).

Li, X.S., Yang, D.Y., Lu, H.Y., Han, H.Y., 1997. The grain-size features of Quaternary aeolian-dust deposition sequence in south Anhui and their significance. *Mar. Geol. Quat. Geol.* 17, 73–87 (in Chinese with English abstracts).

Li, X.S., Yang, D.Y., Han, H.Y., 1998. A preliminary study on the magnetic susceptibility of aeolian-dust deposition-paleosol sequence in the south of Anhui Province. *Journal of Anhui Normal University (Natural Science)* 21 (1), 64–69.

Lin, C.W., Hsue, Z.Y., Chen, Z.S., 2002. Clay mineralogy of Spodosols with high clay contents in the subalpine forests of Taiwan. *Clay Clay Miner.* 50 (6), 726–735.

Liu, T., 1985. Loess and the Environment. Science Press, Beijing (in Chinese, 347 pp).

Liu, Y., Zong, K., Kelemen, P.B., Gao, S., 2008. Geochemistry and magmatic history of eclogites and ultramafic rocks from the Chinese continental scientific drill hole: subduction and ultrahigh-pressure metamorphism of lower crustal cumulates. *Chem. Geol.* 247 (1–2), 133–153.

Mahaney, W.C., Hamilton, T.S., Barendregt, R.W., Hancock, R.G.V., Costa, P., 2014. Mineralogy and chemistry of Late Pliocene–Early Pleistocene paleosols on Mount Kenya: weathering indices of relative age and paleoenvironmental reconstruction. *Geomorphology* 204 (1), 217–228.

Marković, S.B., Hambach, U., Catto, N., Jovanović, M., Buggle, B., Machalett, B., Zöller, L., Glaser, B., Frechen, M., 2009. Middle and Late Pleistocene loess sequences at Batajnica, Vojvodina, Serbia. *Quat. Int.* 198 (1), 255–266.

McCartan, L., 1989. *Geology and paleontology of the Haynesville Cores Northeastern Virginia coastal plain*. United States Geological Survey Professional Paper, p. 1489.

Meunier, A., 2007. Soil hydroxy-interlayered minerals: a re-interpretation of their crystallochemical properties. *Clay Clay Miner.* 55 (4), 380–388.

Millot, G., 1970. *Geology of Clays: Weathering, Sedimentology, Geochemistry*. Springer Verlag, Paris.

Nedachi, Y., Nedachi, M., Bennett, G., Ohmoto, H., 2005. Geochemistry and mineralogy of the 2.45 Ga Pronto paleosols, Ontario, Canada. *Chem. Geol.* 214 (1), 21–44.

Négré, P., 2006. Water-granite interaction: clues from strontium, neodymium and rare earth elements in soil and waters. *Appl. Geochem.* 21 (8), 1432–1454.

Nesbitt, H.W., Young, G.M., 1982. Early Proterozoic climates and plate motion inferred from major element chemistry of lutes. *Nature* 299, 715–717.

Nesbitt, H.W., Young, G.M., 1984. Prediction of some weathering trends of plutonic and volcanic rocks based on thermodynamic and kinetic considerations. *Geochim. Cosmochim. Acta* 48 (48), 1523–1534.

Nesbitt, H.W., Young, G.M., 1989. Formation and diagenesis of weathering profiles. *J. Geol.* 97 (2), 129–147.

Nesbitt, H.W., Markovics, C., Price, R.C., 1980. Chemical processes affecting alkalis and alkaline earths during continental weathering. *Geochim. Cosmochim. Acta* 44 (11), 1659–1666.

Olsen, L., 1998. Pleistocene paleosols in Norway: implications for past climate and glacial erosion. *Catena* 34 (1), 75–103.

Perederij, V.I., 2001. Clay mineral composition and palaeoclimatic interpretation of the Pleistocene deposits of Ukraine. *Quat. Int.* 76, 113–121.

Petersen, L., Rasmussen, K., 1980. Mineralogical composition of the clay fraction of two fluvo-glacial sediments from East Greenland. *Clay Miner.* 15, 135–145.

Qiao, Y., Guo, Z., Hao, Q., Wu, W., Jiang, W., Yuan, B., Zhang, Z., Wei, J., Zhao, H., 2003. Loess-soil sequences in southern Anhui Province: magnetostratigraphy and paleoclimatic significance. *Chin. Sci. Bull.* 48 (19), 2088–2093.

Qiao, Y., Hao, Q., Peng, S., Wang, Y., Li, J., Liu, Z., 2011. Geochemical characteristics of the eolian deposits in southern China, and their implications for provenance and weathering intensity. *Palaeogeogr. Palaeoclimatol. Palaeoecol.* 308 (3–4), 513–523.

Ren, L., 1988. Intermediate structures of clay mineral during transformation. *Acta Sedimentol. Sin.* 6 (1), 80–88 (in Chinese with English abstracts).

Rutter, N., Zhongli, D., Evans, M.E., Yuchun, W., 1990. Magnetostratigraphy of the Baoji loess-paleosol section in the north-central China Loess Plateau. *Quat. Int.* 7, 97–102.

Sawhney, B.L., 1989. Interstratification in layer silicates. *Miner. Soil Environ.* 2, 789–828.

Shackleton, N.J., Opdyke, N.D., 1973. Oxygen isotope and paleomagnetic stratigraphy of equatorial Pacific core V28–238: oxygen isotope temperatures and ice volumes on 106 yr scale. *Quat. Res.* 3, 39–55.

Sheldon, N.D., Tabor, N.J., 2009. Quantitative paleoenvironmental and paleoclimatic reconstruction using paleosols. *Earth Sci. Rev.* 95 (1–2), 1–52.

Sheldon, N.D., Retallack, G.J., Tanaka, S., Sheldon, N.D., Retallack, G.J., Tanaka, S., 2002. Geochemical climofunctions from North American soils and application to paleosols across the Eocene–Oligocene boundary in Oregon. *J. Geol.* 110, 687–696.

Singer, A., 1980. The Paleoclimatic interpretation of clay minerals in soil and weathering profiles. *Earth-Sci. Rev.* 15 (4), 303–326.

Srodon, J., 1999. Nature of mixed-layer clays and mechanisms of their formation and alteration. *Annu. Rev. Earth Planet. Sci.* 27 (1), 19–53.

Vali, H., Hesse, R., 1992. Identification of vermiculite by transmission electron microscopy and X-ray diffraction. *Clay Miner.* 27 (2), 185–192.

Vanderaverdot, P., 1996. Contrôle climatique de la sédimentation argileuse cénozoïque sur la marge passive du New Jersey: Université de Lille I, France.

Vanderaveroet, P., Averbuch, O., Deconinck, J., Chamley, H., 1999. A record of glacial/interglacial alternations in Pleistocene sediments off New Jersey expressed by clay mineral, grain-size and magnetic susceptibility data. *Mar. Geol.* 159 (1), 79–92.

Vanderaveroet, P., Bout-Roumazeilles, V., Fagel, N., Chamley, H., Deconinck, J.F., 2000. Significance of random illite-vermiculite mixed layers in Pleistocene sediments of the northwestern Atlantic Ocean. *Clay Miner.* 35 (4), 679–691.

Velde, B., Meunier, A., 2008. The Origin of Clay Minerals in Soils and Weathered Rocks. Springer-Verlag New York Inc., Berlin.

Walker, 1975. Vermiculite. In: Geisking, J.E. (Ed.), *Soil Components: Volume 1, Inorganic Components*. Springer-Verlag, New York, pp. 155–189.

Weaver, C.E., 1989. Clays, Muds, and Shales: Development in Sedimentology 44. Elsevier, Amsterdam, p. 819.

Wilson, M.J., 1999. The origin and formation of clay minerals in soils; past, present and future perspectives. *Clay Miner.* 34 (1), 7–25.

Wilson, M.J., 2004. Weathering of the primary rock-forming minerals: processes, products and rates. *Clay Miner.* 39 (3), 233–266.

Xi, C.F., 1965. Some problems of Chinese red residuum. *Chin. Quat. Sci.* 4 (2), 42–54 (in Chinese with English abstracts).

Xiao, J., Porter, S.C., An, Z., Kumai, H., Yoshikawa, S., 1995. Grain size of quartz as an indicator of winter monsoon strength on the Loess Plateau of central China during the last 130,000 yr. *Quat. Res.* 43 (1), 22–29.

Xiong, S.F., Liu, T.S., Ding, Z.L., 2000. The weathering sequence of the red earth over southern China. *J. Mt. Sci.* 18 (1), 7–12.

Xiong, S., Sun, D., Ding, Z., 2002. Aeolian origin of the red earth in southeast China. *J. Quat. Sci.* 17 (2), 181–191.

Yang, D., Han, H., Zhou, L., Fang, Y., 1991. Eolian deposit and environmental change of middle-late Pleistocene in Xuancheng, Anhui Province south of the lower reaches of the Changjiang River. *Mar. Geol. Quat. Geol.* 11 (2), 97–104 (in Chinese with English abstracts).

Yang, H., Li, X.P., Zhao, Q.G., Xia, Y.F., 1995. Characteristics of $\delta^{13}\text{C}$ of organic matter in Xuancheng eolian sediment and red earth series profile. *Acta Pedol. Sin.* 32, 177–183 (in Chinese with English abstracts).

Yang, S.Y., Li, C.X., Yang, D.Y., Li, X.S., 2004. Chemical weathering of the loess deposits in the lower Changjiang Valley, China, and paleoclimatic implications. *Quat. Int.* 117 (1), 27–34.

Yang, X., Zhu, Z., Zhang, Y., Li, H., Zhou, W., Yang, J., 2008. Rock magnetic properties and palaeomagnetic results of sediments from a stone implement layer in the Bose Basin, Guangxi. *Sci. China Ser. D Earth Sci.* 51 (3), 441–450.

Yin, Q., Guo, Z., 2006. Mid-Pleistocene vermiculated red soils in southern China as an indication of unusually strengthened East Asian monsoon. *Chin. Sci. Bull.* 51 (2), 213–220.

Yin, K., Gao, Song, E., 2012. Clay mineralogical and geochemical records of paleoclimate in Linxia since the last interglacial. *Acta Pedol. Sin.* 42 (9), 246–259 (in Chinese with English abstracts).

Yin, K., Hong, H., Churchman, G.J., Li, R., Li, Z., Wang, C., Han, W., 2013. Hydroxy-interlayered vermiculite genesis in Jiujiang late-Pleistocene red earth sediments and significance to climate. *Appl. Clay Sci.* 74, 20–27.

Yin, K., Hong, H., Churchman, G.J., Li, Z., Han, W., Wang, C., 2014. Characterisation of the hydroxy-interlayered vermiculite from the weathering of illite in Jiujiang red earth sediments. *Soil Res.* 52 (6), 554–561.

Zhao, Q., Yang, H., 1995. A preliminary study on red earth and changes of Quaternary environment in south China. *Quat. Sci.* 15, 107–115.

Zhou, L.P., Oldfield, F., Wintle, A.G., Robinson, S.G., Wang, J.T., 1990. Partly pedogenic origin of magnetic variations in Chinese loess. *Nature* 346 (6286), 737–739.

Zhu, L.D., Zhou, S.Z., Ye, W., Hu, X., Zhan, X.L., 2005. Study on the red earth sediment and environmental changes in South China. *Journal of Zhejiang Normal University (Natural Sciences)* 28, 206–210 (in Chinese with English abstracts).